

12

INJURY SCIENCE RESEARCH
Proceedings of the Twenty-Eighth International Workshop

Analysis of Air Bag Loads by Inverse Dynamics

P. C. Chan, W. Shen and F. A. Bandak

ABSTRACT

An inverse dynamics method for calculating external air bag loads on the head and neck of a small female test dummy using recorded dummy response data is presented. Calculations were performed for static out-of-position (OOP) tests as well as vehicle crash tests. The calculated external loads provide a phenomenological explanation of the differences in dummy responses between OOP positions 1 and 2. Calculated results for the head-on crash tests show that the bag impact angle on the head affects the head/neck joint load significantly. The upper head/neck joint N_{ij} correlates with the calculated bag impact angle on the head. More chin-up bag impact on the head increases the head/neck moment and N_{ij} . The results demonstrate that inverse dynamics is a useful tool for analyzing dummy test data to help advance the understanding of the air bag external load behavior and bag-occupant interaction.

INTRODUCTION

Air bags have become part of a standard occupant protection system in vehicle crashes, but research based on well-guided physical principles, is still needed to further improve understanding to help minimize injury. Air bags provide a cushion within a short time for the occupant against hard impact during a crash. Concerns have been recognized that the violent deployment of the air bag may cause injury to small occupants that are too close to the air bag, commonly known as out-of-position (OOP) situations (Patrick and Nyquist, 1972; Sullivan et al., 1992; Lau et al., 1993; Mertz et al., 1995; Yoganandan et al., 1995; Johnston et al., 1997). Upper body injuries can result from excessive head accelerations, head/neck joint loads and thorax compression.

Air bag tests generally measure dummy responses that provide very limited information for the relationship between external load and dummy responses. Air bags from the same model year (MY) can produce a great variation of dummy responses. However, there is a limited understanding of how the loads from different air bags are developed to result in widely different dummy responses. Recent work has pointed out the importance of understanding the relationship between load and inflation characteristics based on well controlled and repeatable laboratory method (Bandak et al.). There is still a lack of direct understanding of bag-dummy interaction dynamics.

Besides inflation, the air bag load also depends on such conditions as the bag impact angle, impact location, contact area, bag unfolding pattern and occupant movement. Analyzing these bag-occupant interaction dynamics effects requires external load data. The dummy response data alone do not explain

how these factors relate to load and hence occupant hazard. There is a need to obtain more load information to help understand air bag interaction, evaluate new designs and guide future research in advanced air bag technologies.

The objective of this work is to demonstrate the use of inverse dynamics to calculate external loads on the occupant head and neck using dummy response data from static or crash tests. An inverse dynamics model for the upper body was constructed. Calculations were performed for both static OOP tests and crash tests. Calculated results are used to explain the relationship between dummy head/ neck response and external load behavior.

METHODS

A planar two-dimensional (x-z) model was developed and used as well to analyze frontal impact tests assuming symmetry about the anterior-posterior plane. Figure 1 shows the schematic diagram of the head, neck and torso of a dummy in their local coordinate systems. The head, neck and upper torso are modeled as rigid bodies connected by the upper and lower head/neck joints (Figure 1). The definition and sign convention of the global and local coordinates follow SAE J1980 and SAE J211. The head/neck joint load cells are mounted on the neck with joint loads recorded in the neck frame.

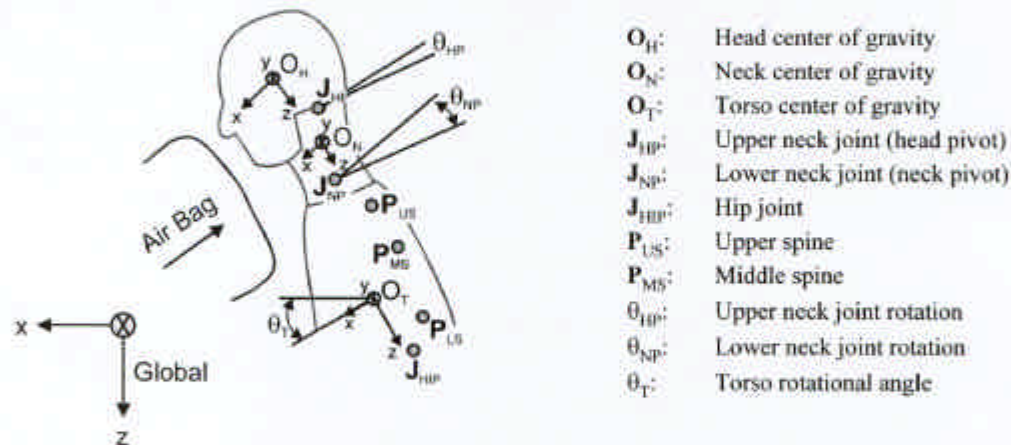


Figure 1. Schematics of head/neck-torso system.

The head/neck model requires boundary condition at the lower head/neck joint that is related to the translation and rotation of the upper torso. The external forces and moments delivered to the head and neck can be calculated using inverse dynamics if the kinetic data (force and moment) at the upper and lower head/neck joints and the kinematics data (acceleration) of the head, neck and chest are available. In most tests using dummies, forces and moments at the head/neck joints are measured, but not all the required kinematics data are always available. Linear accelerations at the center of gravity (CG) of the head and chest are usually measured, while angular accelerations are not. In some tests, linear accelerations at the upper, middle and lower spine locations are measured (Figure 1). Therefore, some kinematics reconstruction may be necessary to estimate the missing angular kinematics information before a full inverse dynamics calculation is carried out.

Based on force and moment conservation, the following vector equations are used to calculate the resultant external air bag forces and moments on the head and neck in their local coordinates.

$$\mathbf{F}_H = m_H \mathbf{a}_H - (\mathbf{R}_{HP})^T \mathbf{F}_{HP} \quad (1a)$$

$$\mathbf{M}_H = I_H \boldsymbol{\alpha}_H - \mathbf{M}_{HP} - \mathbf{v}_1 \times [(\mathbf{R}_{HP})^T \mathbf{F}_{HP}] \quad (1b)$$

$$\mathbf{F}_N = m_N \mathbf{a}_N + \mathbf{F}_{HP} - \mathbf{F}_{NP} \quad (1c)$$

$$\mathbf{M}_N = I_N \boldsymbol{\alpha}_N + \mathbf{M}_{HP} - \mathbf{M}_{NP} + \mathbf{v}_2 \times \mathbf{F}_{HP} \times \mathbf{F}_{NP} \quad (1d)$$

\mathbf{F}_H , \mathbf{M}_H , \mathbf{F}_N and \mathbf{M}_N are the external airbag forces and moments on the head and neck, respectively, with m_H , I_H , m_N and I_N being the masses and moments of inertia, which are obtained from the body property-generating program GEBOD[®] (Cheng *et al.*, 1994). \mathbf{v}_1 , \mathbf{v}_2 , \mathbf{v}_3 are the position vectors from the head CG to the upper neck joint J_{HP} , the neck CG to J_{HP} , and the neck CG to the lower neck joint J_{NP} , respectively, that are also obtained from GEBOD[®]. The upper and lower neck joints are also called the head and neck pivots designated by the subscripts HP and NP (Figure 1). \mathbf{F}_{HP} , \mathbf{M}_{HP} , \mathbf{F}_{NP} and \mathbf{M}_{NP} are the internal forces and moments at the upper and lower neck joints, respectively, which are measured in the neck coordinates. \mathbf{a}_H , $\boldsymbol{\alpha}_H$, \mathbf{a}_N and $\boldsymbol{\alpha}_N$ are the linear and angular accelerations of the head and neck CG, respectively, in their local coordinates. \mathbf{R}_{HP} is the rotational matrix representing that the head frame is related to the neck frame by rotating an angle of θ_{HP} , positive clockwise (Figure 1). Hence, a rotational matrix \mathbf{R} is defined for a rotational angle θ as

$$\mathbf{R} = \begin{bmatrix} \cos(\theta) & -\sin(\theta) \\ \sin(\theta) & \cos(\theta) \end{bmatrix} \quad (2)$$

Calculated head and neck forces can be transformed to global coordinates through successive rotations. Notice that in equation (1), all head and neck quantities are expressed in their corresponding local frames, while the head/neck joint forces are in the neck frame (Figure 1). The calculated air bag forces, \mathbf{F}_H and \mathbf{F}_N , can be transformed into the global frame quantities \mathbf{F}_H^G and \mathbf{F}_N^G by the following equations

$$\mathbf{F}_H^G = \mathbf{R}_T \mathbf{R}_{NP} \mathbf{R}_{HP} \mathbf{F}_H \quad (3a)$$

$$\mathbf{F}_N^G = \mathbf{R}_T \mathbf{R}_{NP} \mathbf{F}_N \quad (3b)$$

where rotational matrices \mathbf{R}_{NP} and \mathbf{R}_T are obtained from equation (2) with $\theta = \theta_{NP}$ and $\theta = \theta_T$ (Figure 1).

Solving equations (1) and (3) requires the angular data of the head, neck and torso, and the linear accelerations of the head and neck. However, in most tests, the angular kinematics of the head and neck and the linear acceleration of the neck are not measured. The reconstruction of these data can be performed in a few steps, beginning with the calculation of the torso rotation.

Upper torso angular acceleration is first reconstructed using chest and/or spine linear acceleration data. If the linear accelerations at two points on the torso are known, the angular acceleration of the torso ($\boldsymbol{\alpha}_T$) can be calculated by dividing the difference of the linear accelerations by their separation distance. If linear accelerations at more than two points are known, the results can be optimized by the minimization of errors, but data are usually insufficient for optimization. Therefore, if the spinal accelerations at P_{US} , P_{MS}

or $P_{1,5}$ are measured, the torso angular acceleration can be calculated using the spinal accelerations and the chest acceleration \mathbf{a}_T . Integrating the angular acceleration twice with respect to time results in the torso rotation angle θ_T . When the spinal accelerations are unavailable, it is assumed that the hip joint J_{HP} behaves like a fixed pivot, and the torso angular acceleration is estimated using the chest acceleration \mathbf{a}_T only.

The rotational kinematics of the head and neck is next obtained in two steps making use of the joint constitutive properties. First, the total head rotation angle (θ_H) with respect to the torso is calculated from the relative position of the head CG to the lower neck joint as follows,

$$\mathbf{a}_{NP:T} = \mathbf{a}_T + \mathbf{v}_i \times \boldsymbol{\alpha}_T \quad (4a)$$

$$\mathbf{a}_{H:NP} = \mathbf{R}_{HP} \mathbf{a}_H - (\mathbf{R}_{NP})^T \mathbf{a}_{NP:T} \quad (4b)$$

$$\mathbf{p}_{H:NP} = \iint \mathbf{a}_{H:NP} dt dt + (\mathbf{v}_i - \mathbf{v}_T - \mathbf{R}_{HP} \mathbf{v}_i) \quad (4c)$$

$$\theta_H = \tan^{-1}(-p_{H:NP}^X / p_{H:NP}^Z) \quad (4d)$$

where $\mathbf{a}_{NP:T}$ is the acceleration of the lower neck joint in the torso frame, and \mathbf{v}_i is the position vector from the torso CG to NP. $\mathbf{a}_{H:NP}$ and $\mathbf{p}_{H:NP}$ are the acceleration and position vector of the head CG relative to the lower neck joint in the neck frame. Then, θ_H is separated into the rotation at the upper neck joint (θ_{HP}) and the lower neck joint (θ_{NP}) in proportion to their joint moments calculated from the joint constitutive relationships. The joint moment M is assumed to be related to the joint angle (θ) and angular velocity (ω) by $M = -k\theta^2 - c\omega$, where k is the rotational spring constant and c is the damping coefficient obtained from GEBOD. Hence, θ_{HP} and θ_{NP} are estimated from the following equations

$$f_{HP} = (-M_{HP} - c_{HP} \omega_{HP}) / k_{HP} \quad (5a)$$

$$f_{NP} = (-M_{NP} - c_{NP} \omega_{NP}) / k_{NP} \quad (5b)$$

$$\theta_{HP} = \text{sgn}(f_{HP}) \frac{\sqrt{|f_{HP}|}}{\sqrt{|f_{HP}|} + \sqrt{|f_{NP}|}} \theta_H \quad (5c)$$

$$\theta_{NP} = \theta_H - \theta_{HP} \quad (5d)$$

The separation of the total head rotation angle into θ_{HP} and θ_{NP} based on the ratio of their estimated magnitudes $\sqrt{|f_{HP}|}$ and $\sqrt{|f_{NP}|}$ as shown in Eq. 5 is heuristic and will be validated against data. Equations

(4) and (5) are solved simultaneously using finite difference, and the calculated angular accelerations of the head and neck (α_H and α_N) are evaluated. The acceleration at the neck CG is

$$\mathbf{a}_N = (\mathbf{R}_{NP})^T \mathbf{a}_{NP-T} - \mathbf{v}_3 \times \alpha_N \quad (6)$$

Inverse dynamics calculations were done after the validation of the kinematics reconstruction method (Eq. 4-6). Four NHTSA static OOP tests conducted with the dummy at position 1 and 2 (Figure 2) were then analyzed. Calculations were carried out for the Transport Canada frontal crash tests for late model vehicles. All tests analyzed used the 5th percentile Hybrid-III small female dummy, and test data were obtained from the NHTSA database.

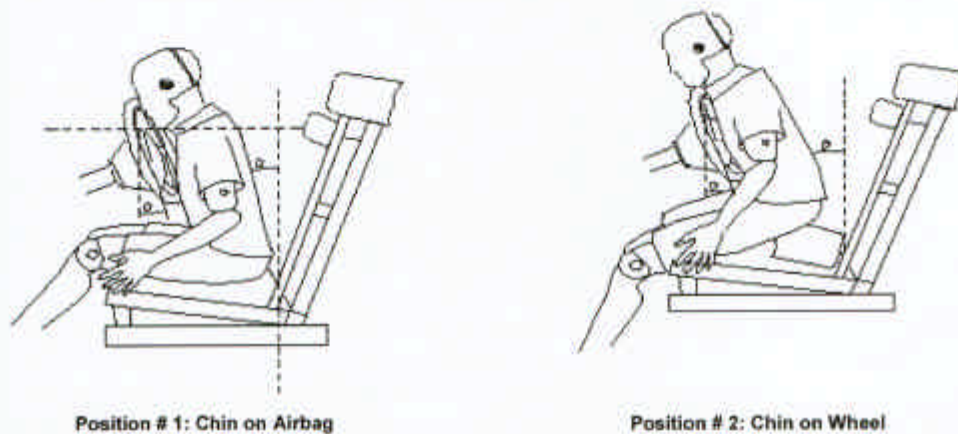


Figure 2. OOP positions for test dummy in NHTSA static tests (Hinch et al., 1999).

RESULTS

NHTSA Static Out-of-Position (OOP) Tests

NHTSA 1998 OOP Test 3783 (Hinch et al., 1999) was used to validate the angular kinematics reconstruction method because this test provided linear acceleration data at the chest and three spine locations, as well as high-speed movies. The torso angular acceleration was calculated in two ways, one using the chest and spinal accelerations, while the other using just the chest acceleration with the fixed hip joint assumption. Visual estimate of the head and torso rotation angles was obtained from the high-speed movies for comparison with the predictions. This test was conducted with the dummy at position 2 (Figure 2). No head/neck joint forces were available for this test.

The rotation angles calculated from Equations 4-5 agree with the high-speed movies (Figure 3). Two selected movie frames at 10 and 75 ms are shown in Figure 3c-d, where the head rotation angle relative to the upper torso are estimated to be 0 and 30 deg, respectively. Since no rotation angle data were available, the estimates using the high-speed movies are assumed to serve as data. As shown in Figure 3a, the calculated torso rotation using both methods are almost identical up to about 110 ms, after which the movie shows that the hip joint starts to develop translational motion, resulting in the divergence

the movie shows that the hip joint starts to develop translational motion, resulting in the divergence between the two predictions. Both predictions of torso rotation agree with the movie estimate up to 110 ms, after which, the prediction using the spine and chest accelerations agrees much better with the data than that with the fixed hip assumption (Figure 3a). The calculated head rotation relative to the torso matches well with data up to 90 milliseconds (Figure 3b). Since significant air bag-dummy interaction generally occurs within 60 ms, the data comparison shows that the kinematics reconstruction method should be adequate for calculating the head/neck rotational accelerations required for the full inverse dynamics simulations within this time frame, even with the fixed hip joint assumption (Figure 3).

Inverse dynamics calculations were performed for NHTSA-UVA static OOP tests T382 and T381 with dummies at positions 1 and 2, respectively (Pilkey 1996a, 1996b). Positions 1 and 2 are generally known as chin-on-bag and chin-on-wheel situations, respectively. The angular head/neck kinematics were reconstructed using the fixed hip joint assumption since spinal acceleration data were not complete. Head/neck joint forces and moments were measured. Calculations were carried out for 60 ms beyond which the air bag load is insignificant. Test data and the calculated air bag load on the head and neck are shown in Figure 4.

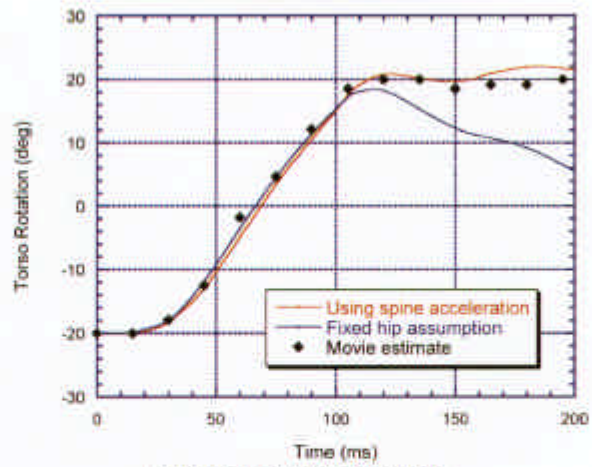
The calculations agree with the data trend that a stronger load is delivered to the head and neck at position 1 than 2 (Figure 4). Figure 4a-h present the measured dummy data and Figure 4i-n present the calculated external loads on the head and neck. The data show that the overall head accelerations and head/neck joint loads are much higher and earlier for position 1 than 2 (Figure 4a-h), and this trend correlates with the calculated external loads (Figure 4i-n). This behavior is reasonable since the air bag hits directly at the head and chin at position 1, while the bag hits the chest first before the head at position 2, as confirmed by the selected frames from the high-speed movies shown in Figure 5.

The total external force magnitude delivered on the head is much faster and stronger for position 1 than 2 (Figure 6). For position 1, as shown in Figure 6, the external load consists of two phases, an early sharp spike peaking to 2.8 kN at 9 ms, and a second slower pulse reaching 2.8 kN at around 30 ms, and the two corresponding movie frames are shown in Figure 5a-b. The initial sharp spike is primarily headward as indicated by the dominant tensional neck joint loads and confirmed by the calculated z-force behavior around 9 ms (Figure 4e, f and k). For test T381 at position 2, the initial pulse rises much slower to 1.5 kN at 18 ms and the second pulse peaks to 1.8 kN at 38 ms (Figure 6), and Figure 5c-d show the two respective movie frames.

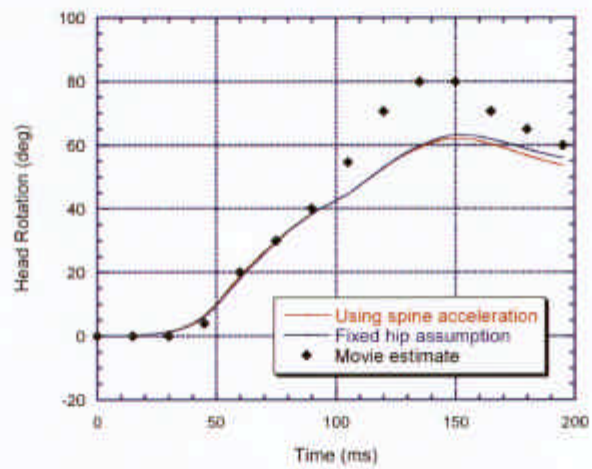
Similar trends of load difference between positions 1 and 2 are also observed from inverse dynamics calculations for NHTSA OOP Test 3777 and 3778, respectively, for a different vehicle. Figure 7a-h present the measured head/neck kinematics data and Figure 7i-n show the calculated external loads. Again, the data and calculations show that higher and earlier loads are delivered to the head at position 1 than 2 (Figure 7), with a trend similar to the T382 and T381 (Figure 4). This trend is confirmed by analyzing the total external force magnitudes on the head for Tests 3777 and 3778 (Figure 8), which are similar to the trend for T382 and T381 shown in Figure 6 for positions 1 and 2, respectively.

Crash Tests

Inverse dynamics calculations were performed to help explain a series of frontal crash tests conducted for late model vehicles by Transport Canada (PMG Technologies, 1998). The dummy was placed in the driver seat at the full forward rail position but was not in OOP situation. Figure 9 presents the recorded dummy head/neck responses in three normalized forms for the head-on test series with 10 vehicles. The



(a) Torso rotation data comparison



(b) Head rotation data comparison



(c) 10 ms



(d) 75 ms

Figure 3. Reconstruction of head and torso rotation for NHTSA OOP test 3783.

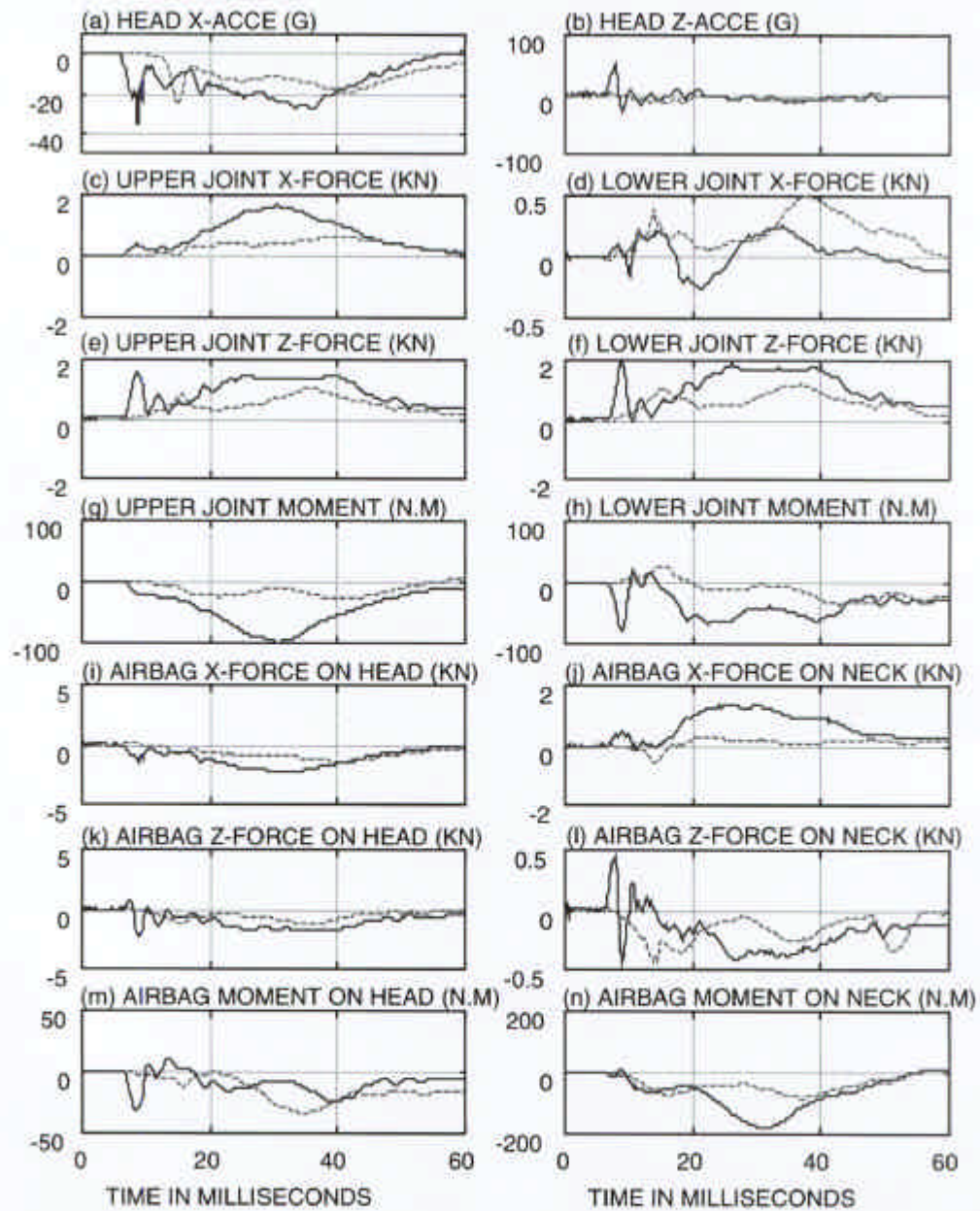
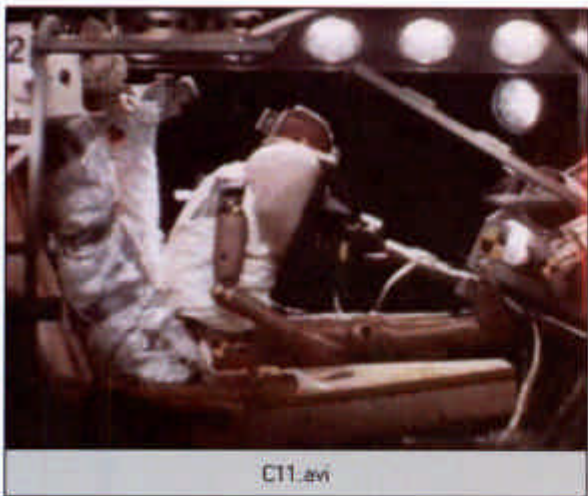


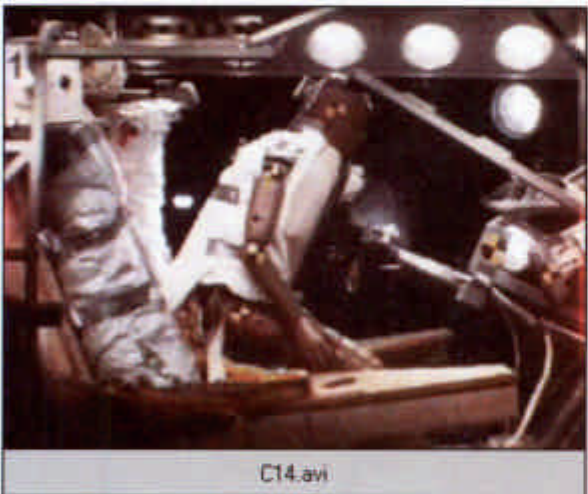
Figure 4. Test data and calculated airbag forces for OOP tests T382 (position-1) and T381 (position-2). (a)-(h): Dummy data; (i)-(n): Calculated external load.



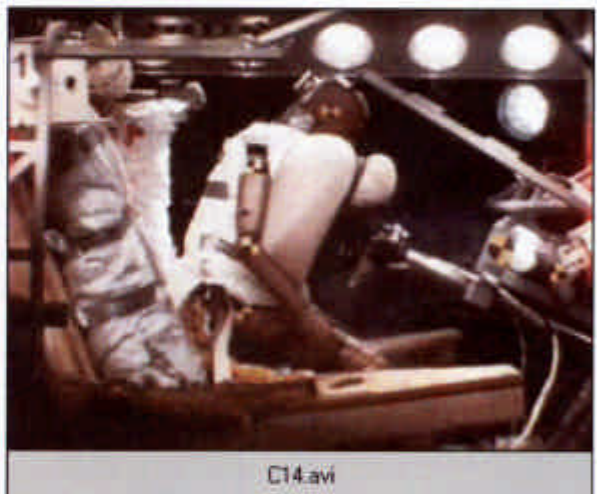
(a) T382, Position 1, Time=9 ms



(b) T382, Position 1, Time=30 ms



(c) T381, Position 2, Time=16 ms



(d) T381, Position 2, Time=38 ms

Figure 5. High-speed movies for test T382 and T381.

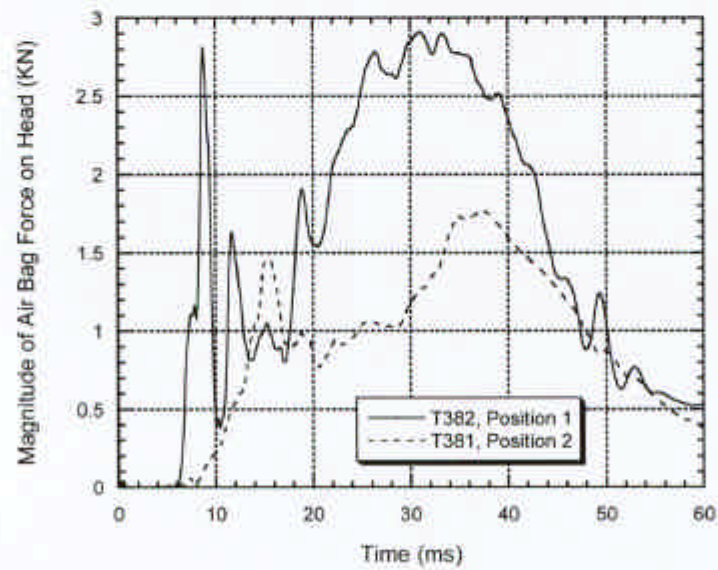
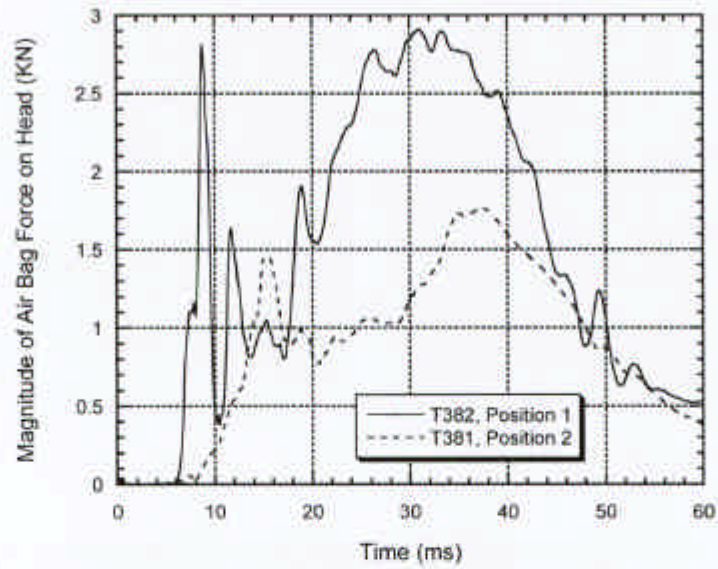


Figure 6. Magnitude of air bag force on head for OOP tests T382 (position-1) and T381 (position-2).

MaxNij is the maximum Nij value is the one used by NHTSA for these tests. Since the dummy head/neck was under tension force F_z and extension bending moment M_y , Nij is

$$N_{ij} = \frac{F_z}{F_{int}} + \frac{M_y}{M_{int}} \quad (7)$$

where F_{int} and M_{int} are the critical intercept values taken as 3370 N and 62 N-m, respectively, and $MaxN_{ij} > 1.4$ may be considered injurious (Eppinger, Sun, Bandak, et al., 1999). The frontal crash tests show that MaxNij exceeds 1.4 for three tests, namely, 3067, 3071 and 3072 (Figure 9). The maximum F_z and M_y are also normalized by F_{int} and M_{int} respectively as shown in Figure 9. MaxNij is dominated by the extensional moment M_y that behaves like a mirror-image (Figure 9). Test 3067 recorded the highest MaxNij of about 2.9 while 3074 resulted in the lowest MaxNij of about 0.5 (Figure 9).

Inverse dynamics calculation results reveal the difference in external loads to the head and neck between tests 3067 and 3074, the high and low head/neck load cases. The kinematics data and calculated external loads are shown in Figure 10a-h and i-n, respectively. Test 3067 recorded stronger head/neck joint forces and moments than 3074 (Figure 10c-h). Especially, the upper head/neck joint force and moment for 3067 are much higher than 3074 (Figure 10c, e and g). Figure 11a-b and 11c-d present selected video frames for 3067 and 3074, respectively corresponding to the times of initial airbag impact and maximum head/neck load. Figure 11a-b show that the 3067 bag hits the head in almost a chin-up fashion. In contrast, the 3074 bag seems to hit almost flatly (horizontal) on the front face of the head and chest simultaneously, pushing the entire head/neck and upper torso backwards together (Figure 11c-d). Indeed, the calculated results show that the 3074 bag delivers a stronger external x-force on the head, while 3067 delivers a stronger z-force (Figure 10i, k). Furthermore, Figure 10j shows that the 3067 bag delivers a 1.1 kN x-force on the dummy neck, which suggests there is significant bag contact with the neck. This seems to agree with the video showing there is potential bag trapping between the chin and neck for 3067, which can cause higher upper head/neck joint moment as indeed measured (Figure 11a-b). In contrast, 3074 resulted in minimal x-force on the neck (Figure 10i), suggesting insignificant neck contact as confirmed by the video (Figure 11c-d).

Analysis of the calculated external load confirms that the bag impact angle on the head strongly affects the head/neck moment. The magnitudes of the calculated total external forces on the head are actually quite similar between tests 3067 and 3074 (Figure 12). The force angles, however, are widely different (Figure 13) where 0 and 90 deg refers to the horizontal and vertical directions, respectively, in the (global) space fixed frame. Figure 12 shows that the bag-head interaction is mostly from 25-100 ms, implying that the force angle beyond 100 ms are immaterial for load considerations. For test 3067, the bag impact angle exceeds 80 deg from 30-70 ms, while for test 3074, the impact angle is mostly less than 35 deg (Figure 13). In other words, although the two bag force magnitudes are comparable, the more chin-up impact for 3067 results in a much higher head/neck moment (Figures 10g, 12-13).

Calculated results for all 10 head-on crash tests confirm that the head/neck moment, hence MaxNij, correlates with the air bag force angle (Figure 14). The three cases with MaxNij exceeding 1.4 indicate force angles exceeding 80 deg (Figure 14 and 9). In contrast, MaxNij is less than 1 when the force angle is below about 50 deg (Figure 14).

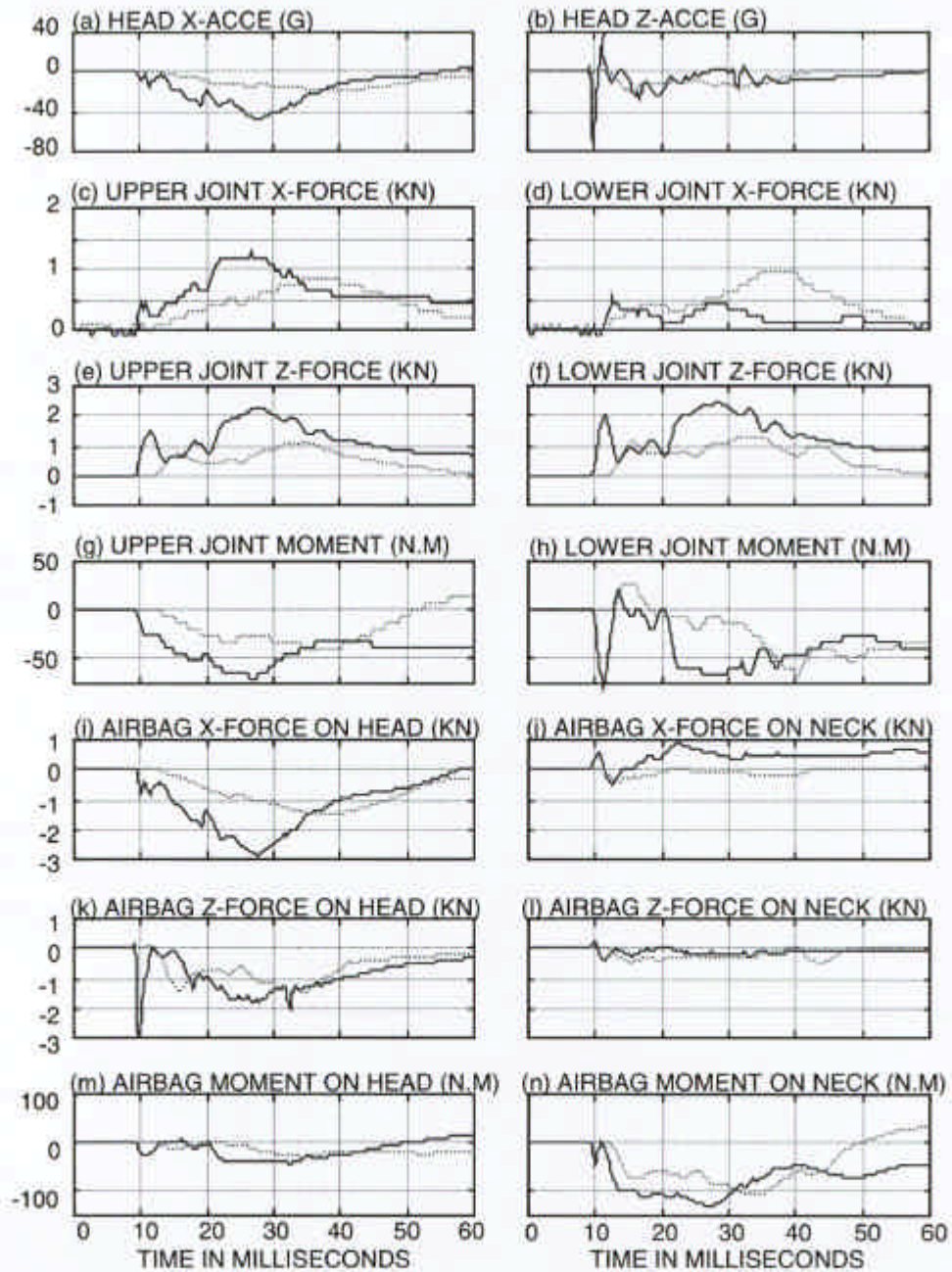


Figure 7. Test data and calculated air bag forces for OOP tests 3777 (position-1) and 3778 (position-2). (a)-(h): Dummy data; (i)-(n): Calculated external load.

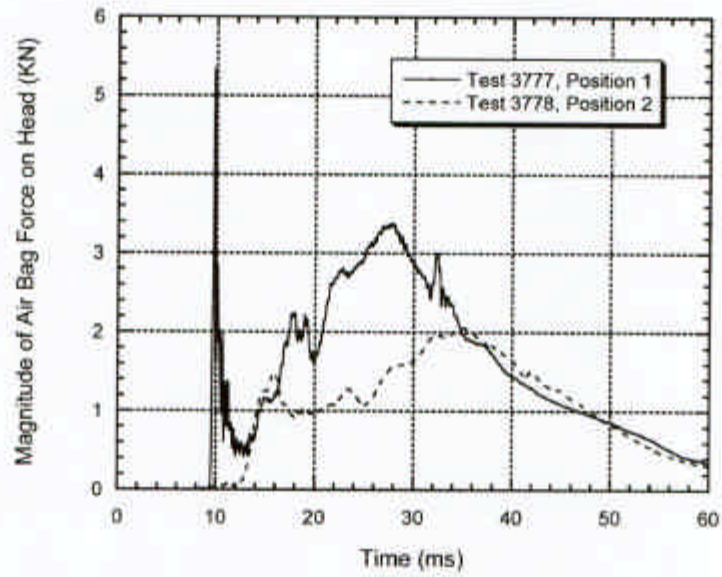


Figure 8. Magnitude of air bag force on head for OOP tests 3777 (position-1) and 3778 (position-2).

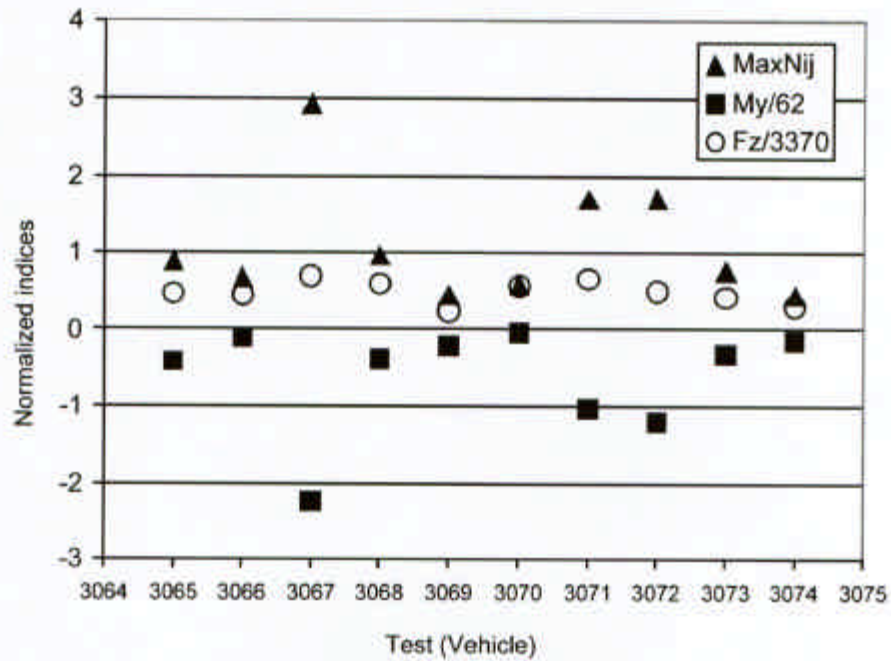


Figure 9. Upper head/neck load data for Transport Canada frontal tests.

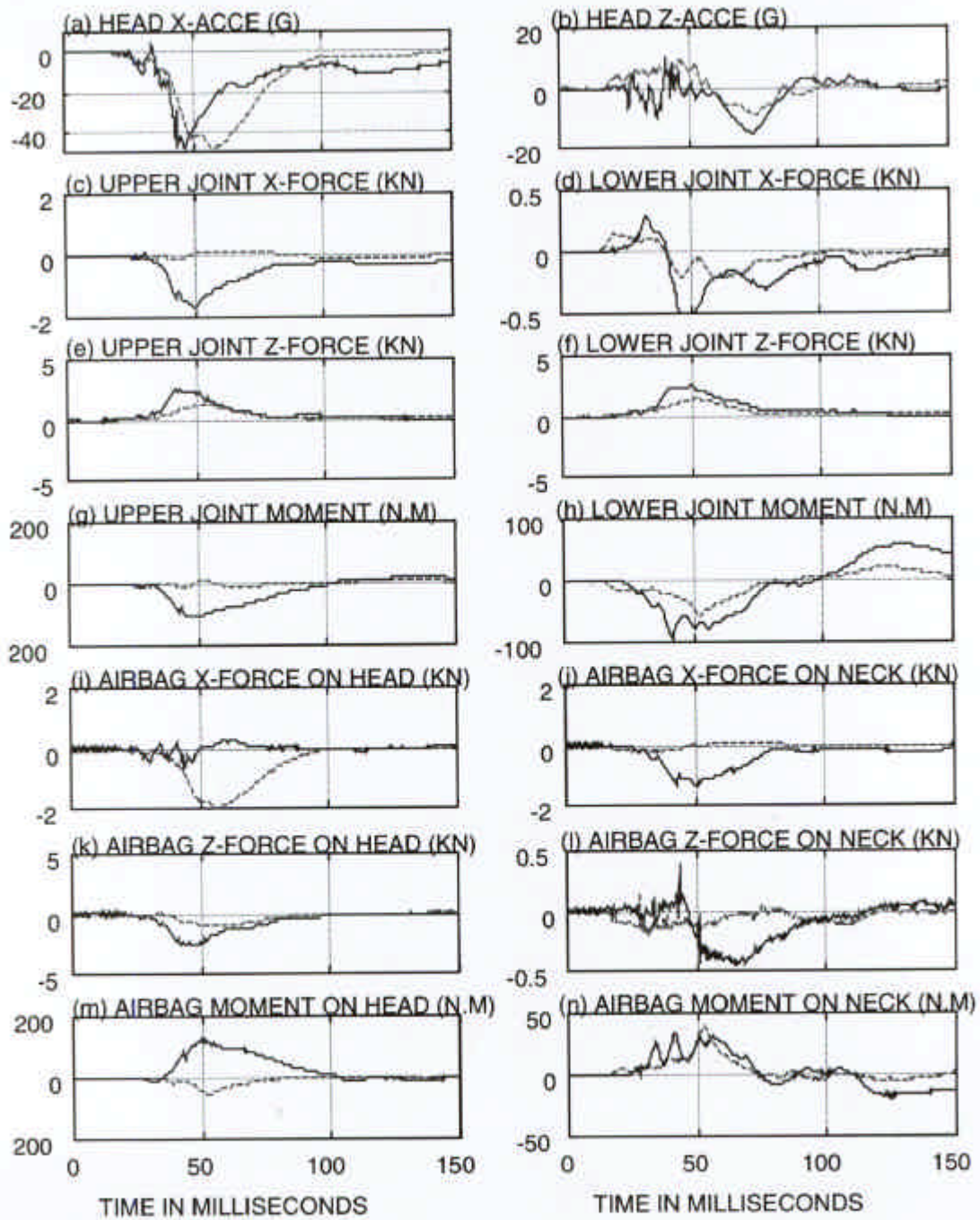


Figure 10. Test data and calculated air bag forces for Transport Canada crash tests 3067 and 3074. (a)-(h): Dummy data; (i)-(n): Calculated external load.

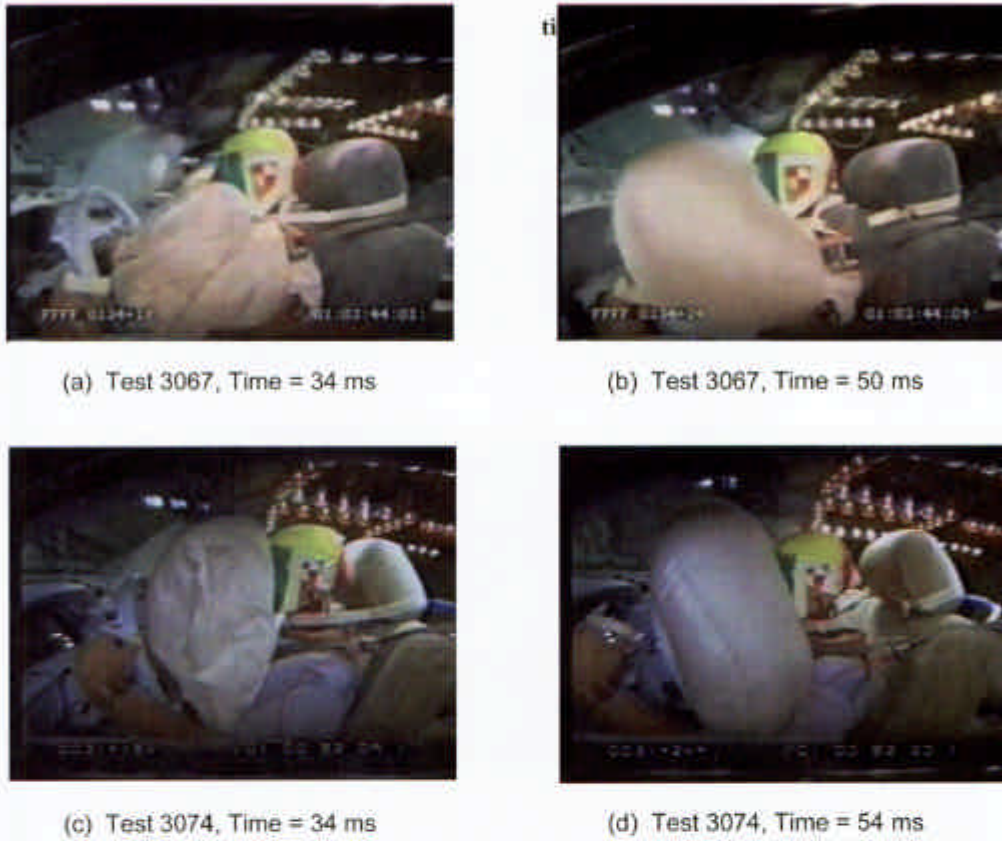


Figure 11. High-speed videos from Transport Canada crash tests 3067 and 3074.

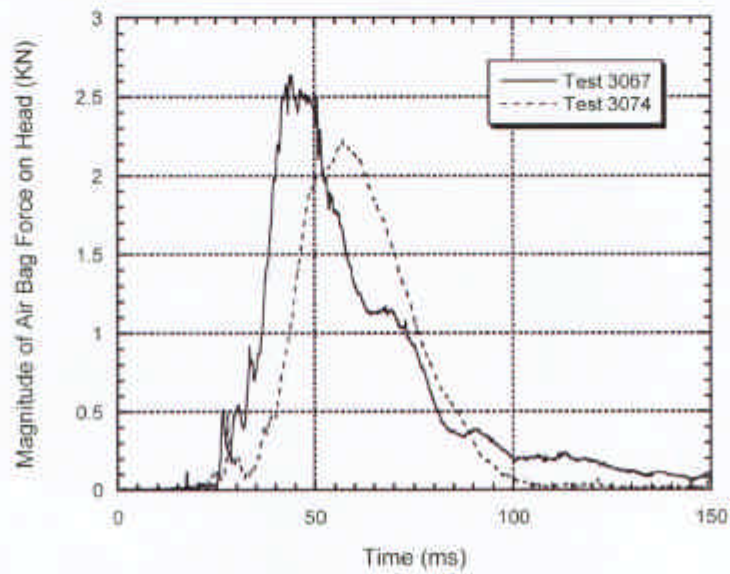


Figure 12. Magnitude of air bag force on head for crash tests 3067 and 3074.

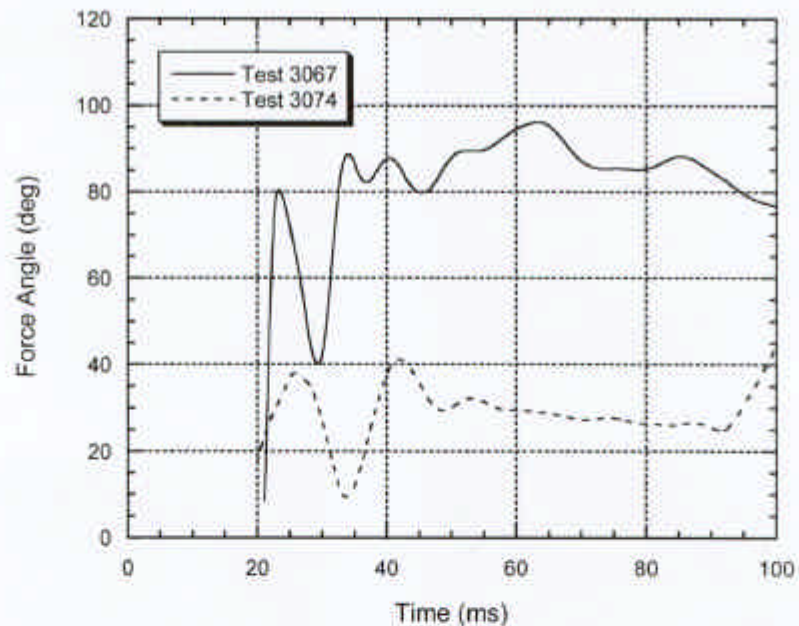


Figure 13. Force angle comparison between tests 3067 and 3074.

DISCUSSION

The present computations assumed the external forces are applied at the CG of the head and neck, although this may not be exactly the case. The resultant external force can be at some other locations with an adjusted external moment. The calculated external forces at the CG can be translated to any other location, but this requires the specification of the head and neck geometry contours and additional criteria not easily defined. Nevertheless, the external force remains unchanged regardless of the point of application. The overall predicted results are considered reasonable, in agreement with the dummy data trends and the high-speed video observations. Direct validation of the inverse dynamic calculations requires a test method to measure the external loads.

It is crucial to account for the rotational effects of the upper torso, neck and head. Model calculations were performed to obtain external loads on the head and neck with the boundary conditions imposed at the lower neck pivot joint (Figure 1). The reconstruction of the chest and neck rotation was to complete the boundary condition specification at the lower head/neck joint. Although, some uncertainties remain, the reconstructed torso and head rotation angles agree with video data. This also suggests that future tests should measure angular data comprehensively.

The chest loads can be calculated by the extension of the demonstrated method. To calculate the chest loads would require more dummy data on the lower extremities, including the hip joint force and moment, seat contact force and seat belt restraint forces. In reality, however, most of these data are not available from air bag tests. Collecting these data will be greatly useful for understanding bag-occupant interaction using inverse dynamics calculations.

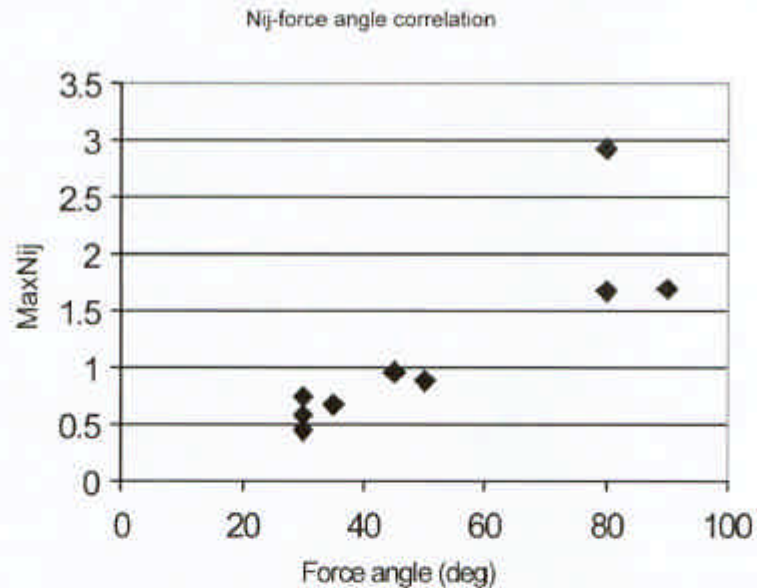


Figure 14. Correlation of Nij with force angle for Transport Canada crash tests.

CONCLUSIONS

An inverse dynamics model has been constructed to calculate external loads on the head and neck due to air bag deployment using dummy response data. A method to reconstruct head/neck and torso angular kinematics has been validated. Inverse dynamics calculations were performed for static OOP tests as well as crash tests. For the NHTSA static OOP tests, calculated results have explained the difference in air bag loads to the head/neck between position 1 and 2, in agreement with recorded dummy load trends and high-speed video observations. Analysis of the Transport Canada head-on crash tests shows that MaxNij correlates with the bag impact angle on the head. It has been demonstrated that inverse dynamics can be a useful tool to analyze test data and help understand the bag-occupant interaction at a fundamental level to advance air bag research and evaluate new air bags.

REFERENCES

- BANDAK, F., CHAN, P. C., HO, K. H. and LU, Z. (2000) "A Method for the Study of Close-Proximity Occupant-Air Bag Interactions," 28th Annual International Workshop on Human Subjects for Biomechanical Research, Atlanta, GA, November 5, 2000
- BASS, C. R., CRANDALL, J. R., and PILKEY, W. D. (1998) "Out-of-Position Occupant Testing (OOPS3 Series), University of Virginia Automobile Safety Laboratory Report OOPS3
- CHENG, H., OBERGEFELL, L. A., and RIZER, A.L. (1994) "Generator of Body (GEBOD) Manual," Report No. AL/CF-TR-1994-0051

- EPPINGER, R., E. SUN, F. BANDAK, M. HAFFNER, N. KHAEWPOONG, M. MALTESE
"Development of Improved Injury Criteria for the Assessment of Advanced Automotive Restraint Systems, NHTSA, September 1998
- HINCH, J. et al. (1999) "Air Bag Technology in Light Passenger Vehicles," Office of Research and Development, NHTSA, Dec. 16, 1999, Rev. 1.
- JOHNSTON, K. L., K. D. KLINICH, D. A. RHULE and R. A. SAUL (1997) "Assessing arm injury potential from deploying air bag," SAE Paper 970400, in "Occupant Protection and Injury Assessment in the Automotive Crash Environment," SP-1231 (SAE, 1997).
- LAU, I. V., J. D. HORSCH, D. C. VIANO, et al., (1993) "Mechanism of injury from air bag deployment loads," *Accid. Anal. Prev.* **25**, 29.
- MELVIN, J. W., HORSCH, J. D., MCCLEARY, J. D., WIDEMAN, L. C., JENSEN, J. L. and WOLANIN, M. J. (1993). "Assessment of air bag deployment loads with the small female Hybrid II dummy," 37th Stapp Car Crash Conference Proceedings, SAE P-269, 1993.
- MERTZ, H. J., G. W. NYQUIST, D. A. WEBER, G. D. DRISCOLL, and J. B. LENOX (1995) "Responses of animals exposed to deployment of various passenger inflatable restraint system concepts for a variety of collision severities and animal positions," SAE Paper 826047, in "Biomechanics of Impact Injuries and Injury Tolerances of the Abdomen, Lumbar Spine and Pelvis Complex," edited by S. Backaitis, (SAE, 1995).
- PATRICK, L., G. NYQUIST (1972) "Airbag effects on the out-of-position child," Second International Conference on Passive Restraints, 1972, SAE Paper 720442, in "Biomechanics of Impact Injuries and Injury Tolerances of the Abdomen, Lumbar Spine and Pelvis Complex," edited by S. Backaitis, (SAE, 1995).
- PILKEY, W. D. (1996a) "UVA Test Report, OOPS ISO-1 Position Series 1 Tests," prepared for NHTSA, Aug. 24, 1996.
- PILKEY, W. D. (1996b) "UVA Test Report, OOPS ISO-2 Position Series 1 Tests," prepared for NHTSA, Aug. 24, 1996.
- PMG TECHNOLOGIES (1998) "Research Frontal Impact, TC 98-014 and 99-215" Tests V3067 and V3074, Transport Canada Safety and Security.
- SAE J1630 (1995) "Driver or Passenger Airbag Module Deployment Test Procedure"
- SAE J1733 (1994) "Sign Convention for Vehicle Crash Testing"
- SAE J198, (1990) "Guidelines for Evaluating Out-of-Position Vehicle Occupant Interaction with Deploying Airbags"
- SAE J211 (1995) "Instrumentation for Impact Test – Part 1: Electronic Instrumentation"
- SULLIVAN, L. K., J. M. KOSSAR (1992) "Air bag deployment characteristics," National Highway Traffic Safety Administration Report No. DOT HS 807 869, February, 1992.

YOGANANDAN, N., F. A. PINTAR, D. SKRADE, W. CHMIEL, J. M. REINARTZ, and A. SANCES, JR. (1993) "Thoracic biomechanics with air bag restraint," SAE Paper 933121, in the *37th Stapp Car Crash Conference Proceedings*, P-269 (SAE, 1993).

